

PAPER • OPEN ACCESS

An Experimental and Numerical Investigation of Heat Transfer Enhancement Using Annular Ribs in a Tube

To cite this article: Mohammed Wahhab Aljibory *et al* 2018 *IOP Conf. Ser.: Mater. Sci. Eng.* **433** 012057

View the [article online](#) for updates and enhancements.

You may also like

- [Analysis on heat transfer calculation of cylinder wall](#)
Yaron Wang and Peirong Wang
- [Numerical Simulation of Heat Transfer Tube Characteristics of Refrigeration and Air Conditioning Based on Mixed Fractional Model](#)
Weihua Ding and Wei Chen
- [Forced Convective Heat Transfer of RP-3 Kerosene at Supercritical Pressure inside a Miniature Tube](#)
Ning Wang and Yu Pan



ECS
The
Electrochemical
Society
Advancing solid state &
electrochemical science & technology

DISCOVER
how sustainability
intersects with
electrochemistry & solid
state science research

An Experimental and Numerical Investigation of Heat Transfer Enhancement Using Annular Ribs in a Tube

Mohammed Wahhab Aljibory¹, Farhan L. Rashid², Shahid M. Abu Alais³

¹ Department of Mechanical.Engineering University of Kerbala,Kerbala,Iraq.

² Department of Petroleum and Petrochemical Engineering.University of Kerbala,Kerbala,Iraq.

³ Department of Mechanical.Engineering University of Kerbala,Kerbala,Iraq.

¹E-Mail: Dr.Mohammad.wahab@uokerbala.edu.iq

²E-Mail: engfarhan71@gmail.com

³E-Mail: shaheedt2017@gmail.com

Abstract

In this study, heat transfer and fluid flow features were numerically and experimentally studied in a circular steel passage of length 50 cm with an outer diameter of 40 mm and inner diameter of 37 mm under a constant surrounding temperature of 673 K for Reynolds numbers $Re=10,800$, $12,900$, and $15,700$, in order to simulate a gas turbine blade cooling passage. Turbulence was simulated using ANSYS - FLUENT (version 16.1), and the (k- ϵ) turbulence model was utilised. The rib constructions (of 5 x 10 mm equilateral triangular cross-section) were fixed inside the circular passage and diverged by 5 cm. The results of temperature and velocity distribution along the circular passage's centreline for the smooth passage were compared with those of a circular passage fitted with these enclosed ribs. An improvement in the rate of heat transfer, especially at $Re=12,900$, was observed in the tube with ribs, with a rate of heat transfer increase of 84.3% compared to the smooth case; the ribbed tube was also observed to have a greater performance factor for turbulent flow.

Keywords: Gas turbine; heat transfer enhancement; rib turbulator; turbulent flow, internal cooling.



Nomenclature

Symbol	Description	Units
A	Area of Surface	m ²
C _p	Air Heat Capacity	J/kg.K
D _h	Hydraulic Diameter	M
E	Height of Rib	M
F	Friction Factor	[-]
G	Acceleration Because of Gravity	m/s ²
H	Coefficient of Heat Transfer	W/m ² .K
K	Thermal Conductivity	W/m.K
L _c	Characteristic Length	M
\dot{m}	Mass Flow Rate	kg/s
M	Air Dynamic Viscosity	N s/ m ²
Nu	Nusselt Number	[-]
P	Rib Spacing (Pitch)	M
Q	Heat Transfer Rate	W
P _w	Circumference	M
Re	Reynolds Number= $\rho u D/\mu$	[-]
T	Temperature	K
U	Flow Velocity	m/s

1. Introduction

Many industrial applications, including aircraft and power plants, use gas turbines [1]. As an effect of modern increased requirements for energy and power, improvements in and increased gas turbine performance is required, and this improvement and increased efficiency may be made by boosting the cooling performance of these gas turbines [2]. When tracking the cooling evolution of turbine feathers, it should be noted that during the past half century, the cooling of the components of gas turbines has been done by force convection of single phase internal flow gas; the interior corridors were initially simple and smooth, then their geometry and surfaces became more complex and rougher [3, 4]. Throughout the years, huge progress has been made in terms of developing air cooling methods to contribute to improving heat transfer [5].

Shukla and Srivastava [6, 7] studied internal cooling by means of air flow in ducts, which is currently very widespread. However, only a finite quantity of air flows are obtainable for such cooling, and more efficacious heat carrying capacity is desired. Drops in pressure also lowers available air flow, thus requiring a highly efficient heat transfer process [8].

One of the important problems in fluid mechanics and thermal science is that of forced turbulent heat convection in rectangular and square channels. In heat transfer devices, rectangular channels are regularly utilised. To improve heat transfer in the flow of cooling air into the duct tabulators, ribs and similar structures have been utilised as excitors of turbulence. The laminar sublayer of the flow is broken by these extraneous elements, and the heat transfer is improved despite the pressure decline, one of the most important parameters in the interpretation of the overall execution of such flows. Several studies have thus attempted to

predict the effectiveness of the number of walls with ribs on friction characteristics and heat transfers [5].

There is a separation of the flow at the head of the rib and a later connection between the ribs. The boundary layer is thus troubled, adding to the disturbance of the flow because of reattachment and separation. When the elements of the fluid mix close to a wall surface, with the cooler ones in the middle of the flow, these two phenomena cause augmentation of heat transfer. Thermal energy is thus transported from the surfaces and external areas of the turbine blades to the interior zones by conduction and that heat is taken away via internal cooling [2]. Increasing turbulence thus improves the heat transfer to the flow of coolants in a duct. These rough areas separate the laminar sub-layer of this flow, and the heat transfer is heightened, as is the pressure drop, which are the major parameters in the study of performance of such flows [5].

Hagari [9] numerically investigated the action of the rib density on the mechanisms of heat transfer enhancement and flow in an internally cooled channel with rib tabulators, establishing a test setup in which the distribution of heat transfer coefficients and flow fields could be predicted using LES methods. The pitch and height rib proportions were 3 and 11, and the Reynolds number depended on Bulk or Mean Velocity. The passage's hydraulic diameter was set at 30,000. A comparison of heat transfer characteristics and time-averaged flow between experimental and numerical results showed that the predictive accuracy of current numerical models was reasonable. The research proposed that, for low-frequency velocity vacillations, larger rib density characterised improved heat transfer. To study the heat transfer mechanism, flow, instantaneous velocity, and temperature domains were compared. For lower rib densities, miniature vortices continuously ensued from each rib and were squandered into the main stream prior to arriving at the following rib. For larger rib densities, large vortexes occurred over the ribs, with supplementary smaller vortexes arising in the gap separating the ribs. The big vortexes happened fitfully after the secondary rib in the duct, gaining in size by combining with smaller vortexes downstream. For each rib pitch, a similar trend was recognisable in the results acquired using Particle Image Velocimetry. This variable vortex construction helped improve the heat transfer of a cooling passage with irregularly arranged rib tabulators.

Metzger and Sham [10] studied heat transfer effects around smooth rectangular channels with sharp, 180° turns. Carlomagno [11] also reported on heat transfer measurements gathered by means of infrared thermography in an internal flow through 180° turns in a square channel, which are relevant to the internal cooling of gas turbine blades. He showed that the Nusselt number increased ahead of the bend, while some very high heat transfer coefficient regions were present at the wall close to the partition wall axis.

Jian et al. [12] discovered that classical ribs offer the smallest advantage, certainly less than annular cylindrical ribs in terms of maximising pressure loss and heat transfer. Thus, circular ribs can boost the flow impingement upstream of the ribs, which increases the areas of heat transfer. The layout of groove and cylindrical annular ribs is also important in terms of enhancing heat transfer and the overall thermal performance of internal passages.

Parkpoom and Paranee [13] studied heat transfer enhancement in heat exchangers by supplying inclined baffles to generate vortexes of co-rotating flows examined using the CFD method with a $k-\epsilon$ model. The circulating fluid was air, flowing in a rectangular passage with a height of 30 mm, and the range of Reynolds numbers was 12,000 to 35,000. The CFD experiment compared a smooth channel and baffled channels (ratios of baffle to channel-height of 0.1, 0.2, and 0.3 and attack angles of 30°, 45°, and 60°). These researchers discovered that Nu and f occurred in a range of -10% to +10%.

Arkan Al Taie et al. [14, 15, 16, 17, 18] presented numerical and experimental research on heat transfer characteristics and thermal performance in 50 cm stainless steel tubes with outer diameters of 60 mm and inside diameters of 30 mm with constant surrounding hot air temperatures of 1000, 1200, and 1400 K using ANSYS Fluent 14.5. The results indicated that the highest performance was achieved in turbulent flow, and that the use of internal ribs increased the rate of heat transfer, causing that enhancement.

In this paper, the effect of fitting triangular cross section rings in a steel tube with internal air flow and a constant wall surface temperature will be investigated numerically and experimentally.

2. Governing Equation

The continuity equation representing the conservation of mass may be written as [19]

$$\dots (1)$$

where ρ represents air density, and the velocity of fluid at selected point in the fluid flow-field is represented by velocity components u , v , and w at x , y , and z , respectively. It is impossible to model turbulent eddies in the fluid flow by direct numerical simulation with current availability of computer resources. Thus, the Cartesian tensor equation for the RANS equations is [20]

$$\frac{\partial u}{\partial x_j} (\rho u_i u_j) = -\frac{\partial P}{\partial x_i} + \frac{\partial}{\partial x_i} \left[\mu \left(\frac{\partial u_i}{\partial x_j} + \frac{\partial u_j}{\partial x_i} - \frac{2}{3} \delta_{ij} \frac{\partial u_i}{\partial x_i} \right) \right] + \frac{\partial}{\partial x_j} (\overline{\rho u'_i u'_j}) \quad \dots (2)$$

With a surface temperature of T_h on one side and T_c on the other side, the heat transfer rate equation due to conduction is:

$$Q = UA(T_h - T_c) \quad \dots (3)$$

From the Nusselt number definition, the Nusselt number of this heat transfer may be calculated as

$$h = \frac{Nuk}{L_c} \quad \dots (4)$$

where L_c is the characteristic length (or hydraulic diameter, D_h), and can be written as

$$D_h = \frac{4A}{P_w} \quad \dots (5)$$

The Reynolds number of fluid flow is expressed as

$$Re = \frac{\rho u D_h}{\mu} \quad \dots (6)$$

turbulent and, as pointed in [1], high Reynolds number k - ϵ models are based on the Boussinesque approximation of Reynolds stresses. Turbulent eddy diffusivity is thus expressed in terms of turbulence parameters k and ϵ . Two additional scalar transport equations, one for turbulent kinetic energy, k , and the other for the turbulence dissipation, ϵ , are therefore solved to model the turbulence effects. The eddy viscosity of this model is obtained by

$$\mu_t = \rho C_\mu \frac{k^2}{\varepsilon} \quad \dots (7)$$

and the k and ε transport equations are

$$\nabla \cdot (\rho k \bar{V} - \frac{\mu_t}{\sigma_k} \nabla k) = P - \rho \varepsilon \quad \dots (8)$$

$$\nabla \cdot (\rho \varepsilon \bar{V} - \frac{\mu_t}{\sigma_\varepsilon} \nabla \varepsilon) = C_1 P \frac{\varepsilon}{K} - C_2 \rho \frac{\varepsilon^2}{k} \quad \dots (9)$$

where P is the usual Reynolds stress turbulence production term, given as

$$P = \mu_t \left[2 \left[\left(\frac{\partial u}{\partial x} \right)^2 + \left(\frac{\partial v}{\partial y} \right)^2 + \left(\frac{\partial w}{\partial z} \right)^2 \right] + \left(\frac{\partial u}{\partial y} + \frac{\partial v}{\partial x} \right)^2 + \left(\frac{\partial u}{\partial z} + \frac{\partial w}{\partial x} \right)^2 + \left(\frac{\partial w}{\partial y} + \frac{\partial v}{\partial z} \right)^2 \right] \dots (10)$$

3. Experimental Procedure

Figure (1(a, b)) explains the chief parts of the test rig which was designed and produced in the laboratories of the Engineering College of Kerbala University, which is also pictured in figure (2). This rig consisted of a circular steel pipe test section, with an air blower connected by an elongated channel with the same cross-section dimensions to the test section passage, which was enclosed in a furnace box in a horizontal layout. The power supplied to the Ni-Cr heating wire was 1000 W, oriented in a uniform manner around the test section channel. The furnace was well insulated with alumina, which offered good thermal insulation in order to avoid heat losses to the surrounding environment. The system included a blower, a heating system, several U-manometers, a control circuit, and K-type thermocouples. The thermocouples' readings were observed every 30 minutes until the steady state condition was achieved. The air flow rate from the blower was controlled with a radiating switch.

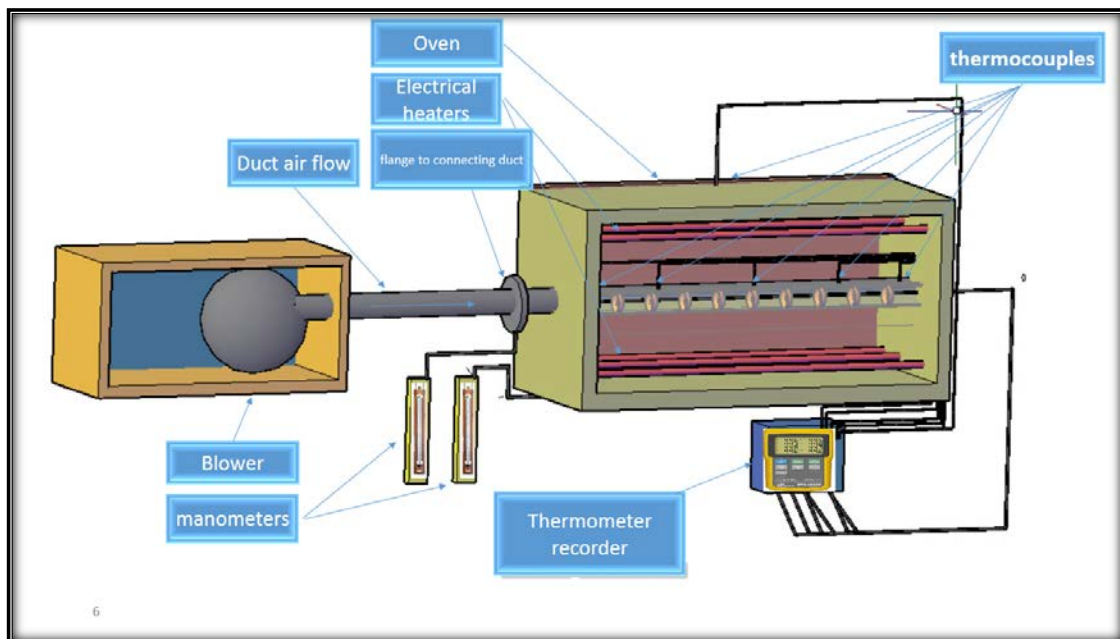


Figure 1.a The experimental setup diagram

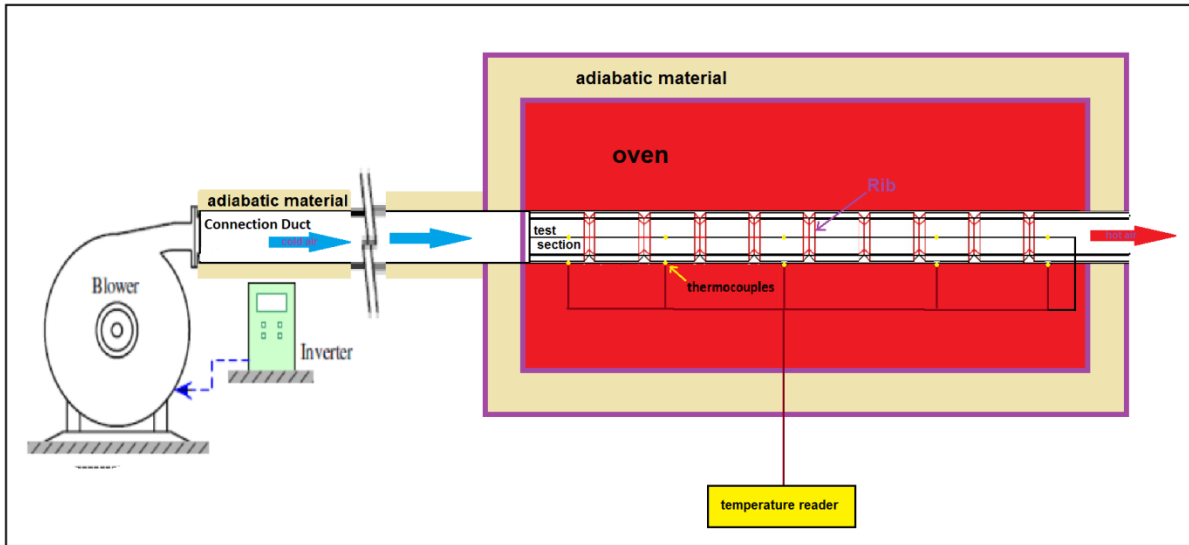


Figure 1.b Schematic diagram of test rig



Figure 2. Photographic view of experimental rig

Annular stainless-steel ribs of a triangular shape were produced, then these were arranged in the 40 mm passage test section using the following method:

1. Holes were made in the surface of the test corridor.
2. Ribs were squeezed using a rod with a 50 mm spacing that was then inserted into the passage to ensure that all the ribs entered the correct position. The ribs were then fixed in place using bolts in the upper surface, as shown in Figure (3).

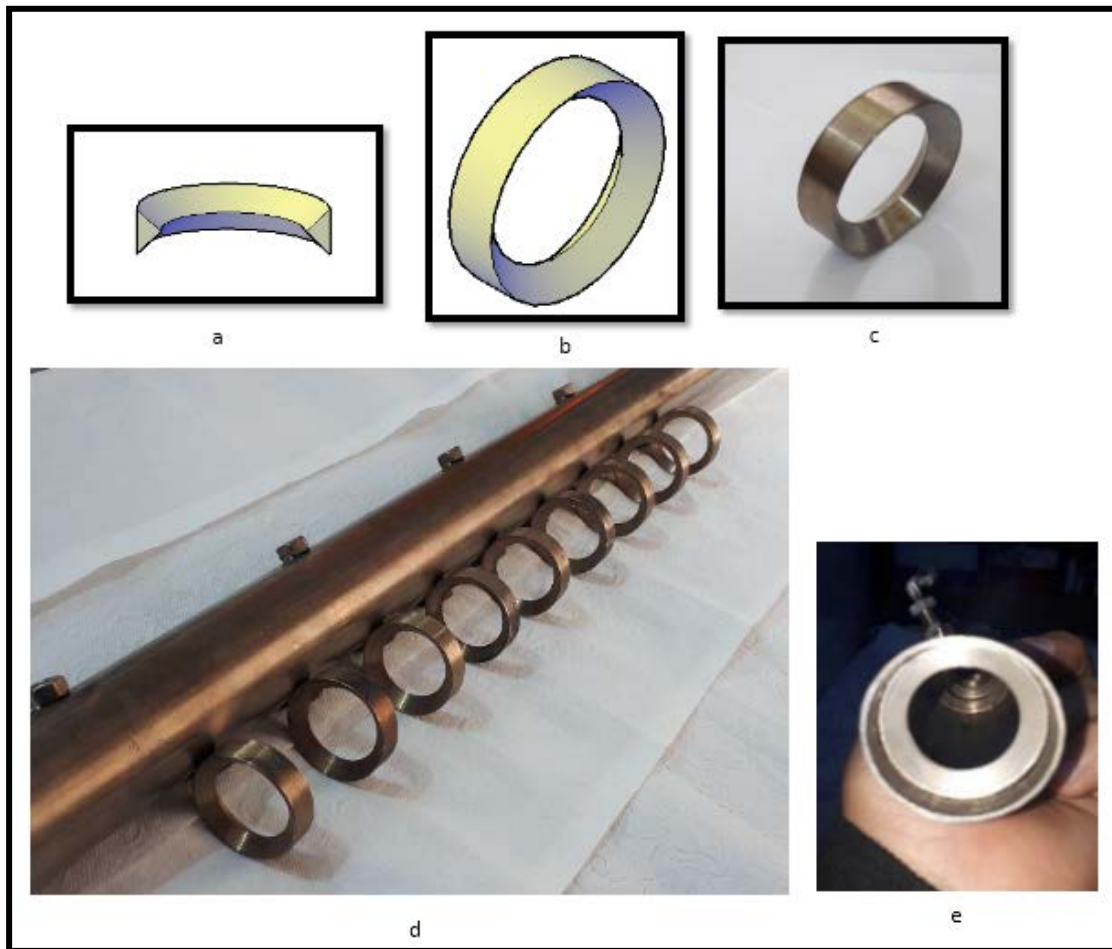


Figure 3. (a, b, c, d, e): View of ribs used in the test: a) cross section of rib; b) three-dimensional view of rib; c) picture of ribs; d) arrangement of ribs inside the passage; e) picture of front view of the ribs inside the passage.

4. CFD Methodology

Three-dimensional simulation was also done in this research. In order to simulate convective heat transfer, the simulation was made in Ansys version 16.1 CFD modelling offered numerical solutions to three type of equations, which were the conservation equations for mass, energy, and momentum. To model the process of convective heat transfer, these three equations were used with three assumptions: (1) heat transfer and fluid flow are steady and 3-D; (2) both fluid and flow are compressible; and (3) the physical properties of cooling fluid are dependent on temperature.

4.1. Boundary conditions:

In the same GAMBIT, the boundary zone location was stipulated, and the wall condition location, outlet, and inlet were specified.

4.2. Fluid entrance boundary condition:

The velocities of inlet air flow at a constant temperature of 300 K were set as 4.7, 5.6, and 6.8 m/s.

4.3. Wall Boundary Conditions:

The wall of the passage was equipped with wall boundary conditions, and 673 k set as the fixed hot temperature for both plain and ribbed circular passages. This work required 700 iterations to reach convergence, as where the residuals did not come below the proper values, additional iterations were requested. The output iterations are shown in Figure (4).

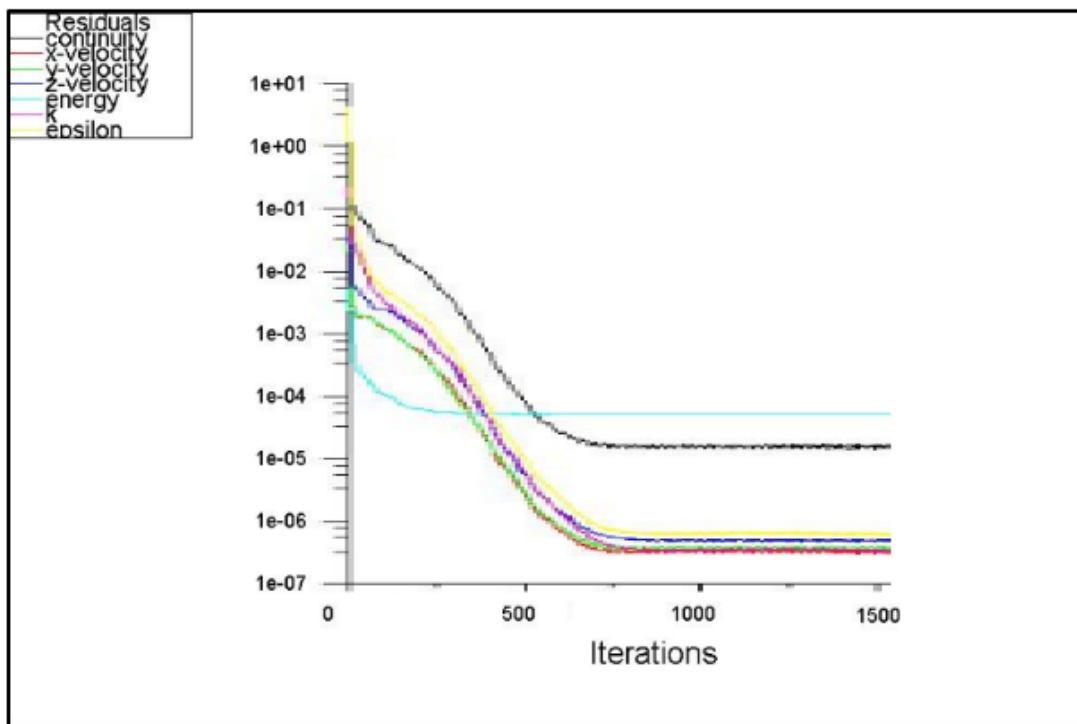
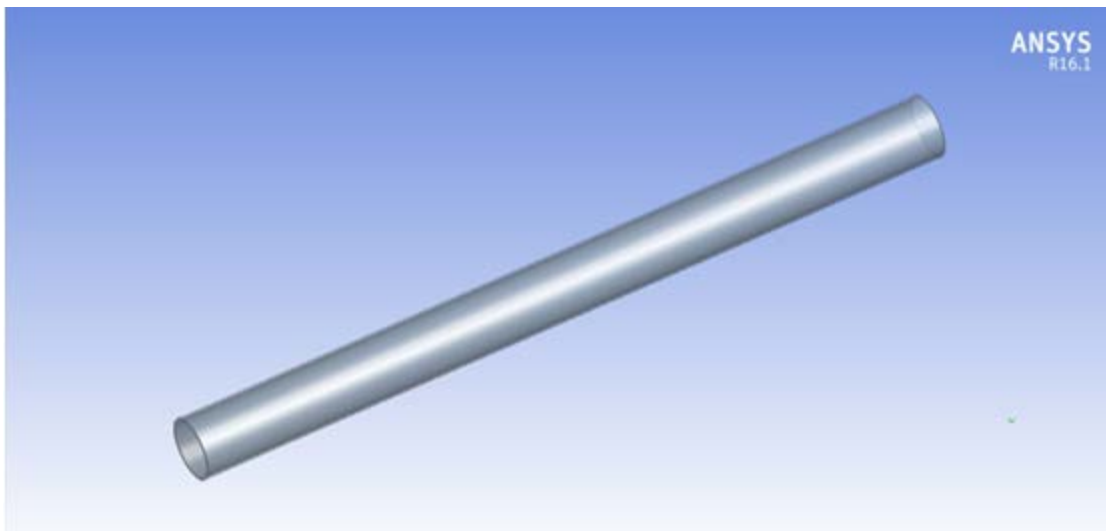


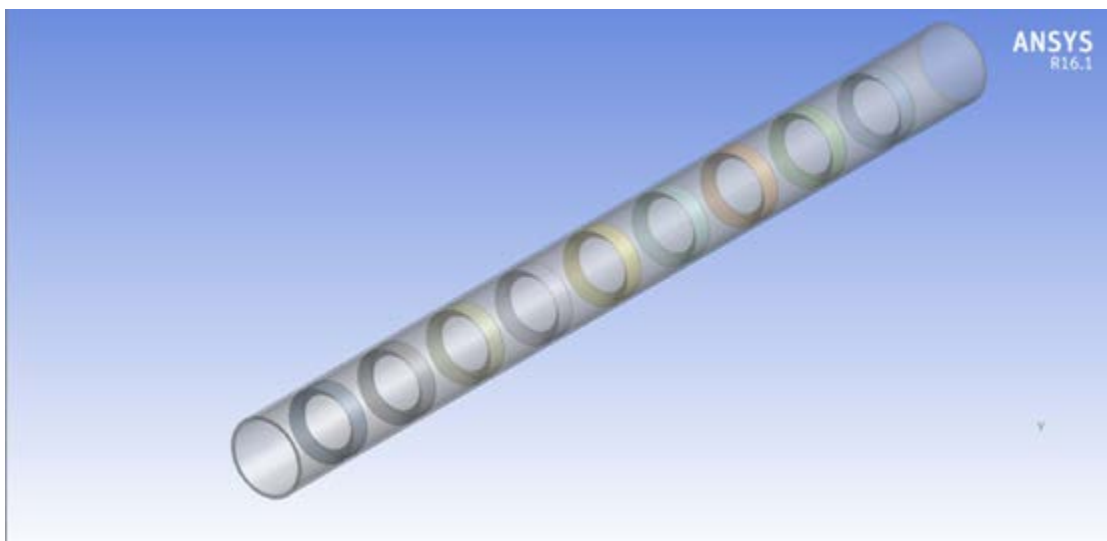
Figure 4. Convergence to solve discrete conservation equations for $Re=12900$

5. Results and Discussion

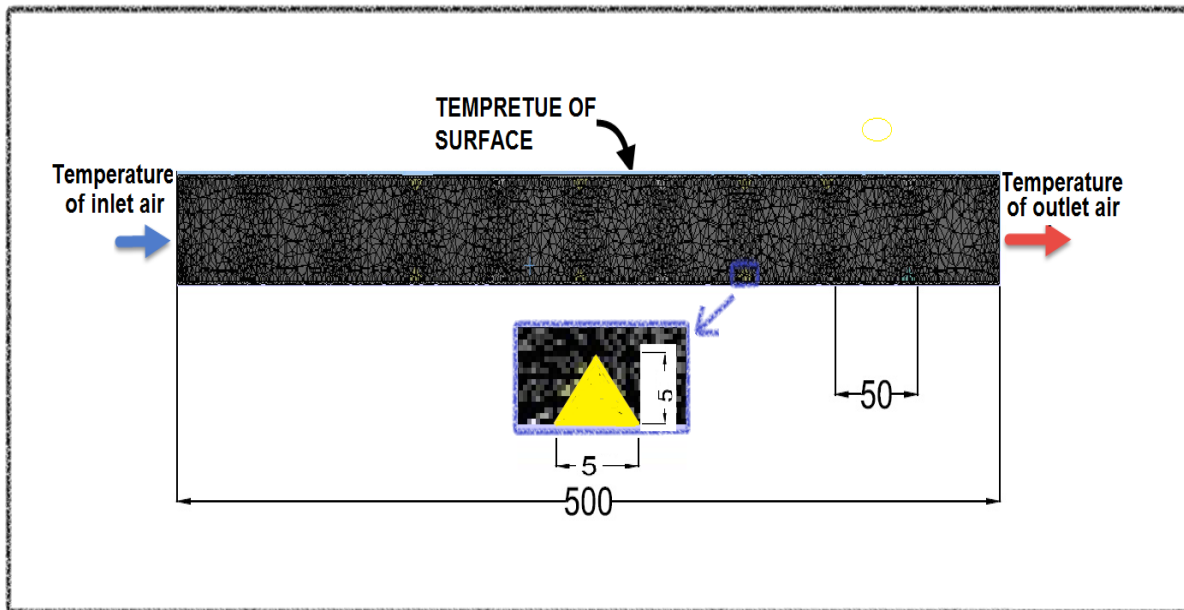
In this research, results were taken for the circular passage compared to the circular passage containing the ribs as presented in Fig. (5: a, b, c).



a)



b)



c)

Figure 5. (a, b, c): a) 3-dimensional view of passage (smooth circular) b) 3-dimensional view of passage (ribbed circular) c) computational domain.

Figures (6) and (7) show the contours of temperature distribution for smooth circular and ribbed cross-section passages, respectively, at a surrounding hot air temperature of 673 K, inlet air temperature 300 K, and coolant air flow with a Reynolds number $Re=12,900$. It was found that the temperature of the cooling air at the traffic line changed slightly, while the temperature of the coolant air near the wall was more greatly affected by the ribs, as shown in Figures (3) and (5), respectively. This is due to the effect on the circulation generated by the ribs, which clearly promotes heat transfer between the cooling fluid flow and the walls of the hot passage.



Figure 6. Temperature distribution for smooth circular passage.

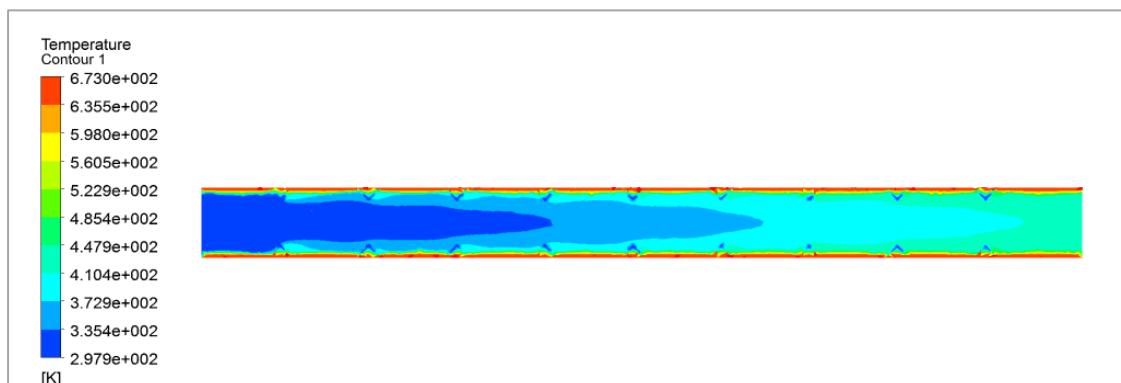


Figure 7. Temperature distribution for ribbed circular passage

Figure (8) shows the experimental cooling air temperatures at the passage centreline for a constant surrounding hot air temperature of 673 K, inlet air temperature of 300 K, and coolant air flows of $Re=10800$, 12900, and 15700. The coolant air temperature at the channel centreline seems to be higher than that seen in the smooth passage (without ribs). Ribs make wakes which develop vortices, and this leads to increases in heat transferred from the passage wall to the cooling air; thus, the increase in coolant air temperature obtained was 10 % for case 1, 9.6 % for case 2, and 8.3% for case 3.

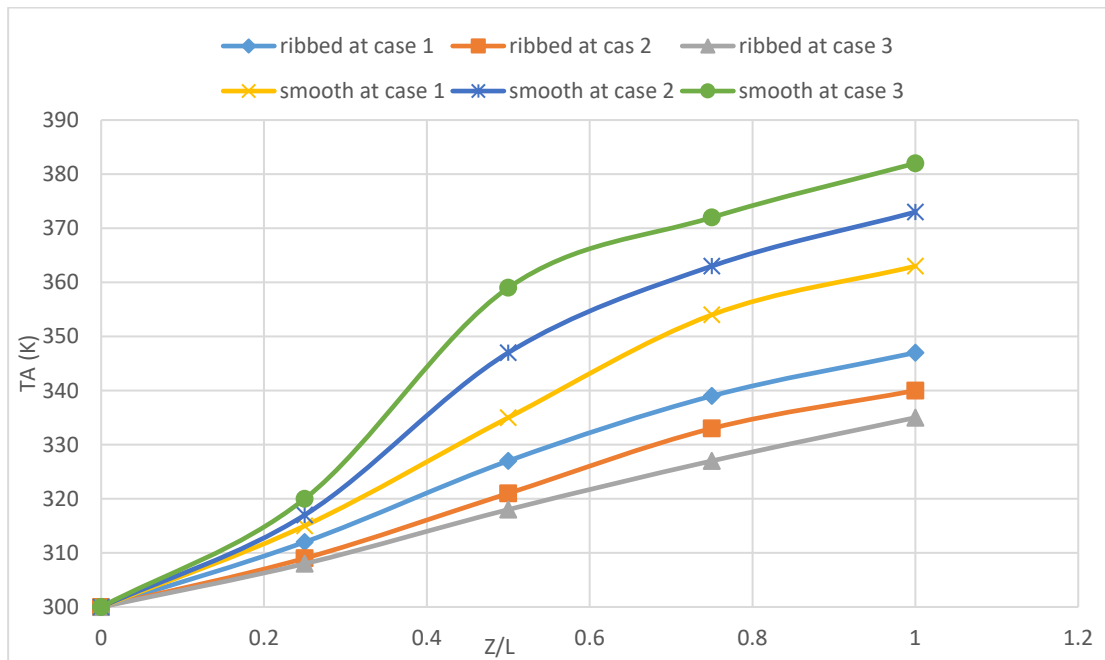


Figure 8. The experimental temperature distribution at passage centreline from experimental test

Figure (9) presents the variation of average Nusselt number with Reynolds number at a constant surrounding air temperature of 673 K. This demonstrates that an increase in Reynolds number raises the average Nusselt number. In addition, each heat transfer process using ribs appears more effective than the smooth passage. This is because using ribs offers more heat transfer than using a plain tube due to reverse flow and boundary layer disruption, which help to enhance the heat transfer and momentum processes.

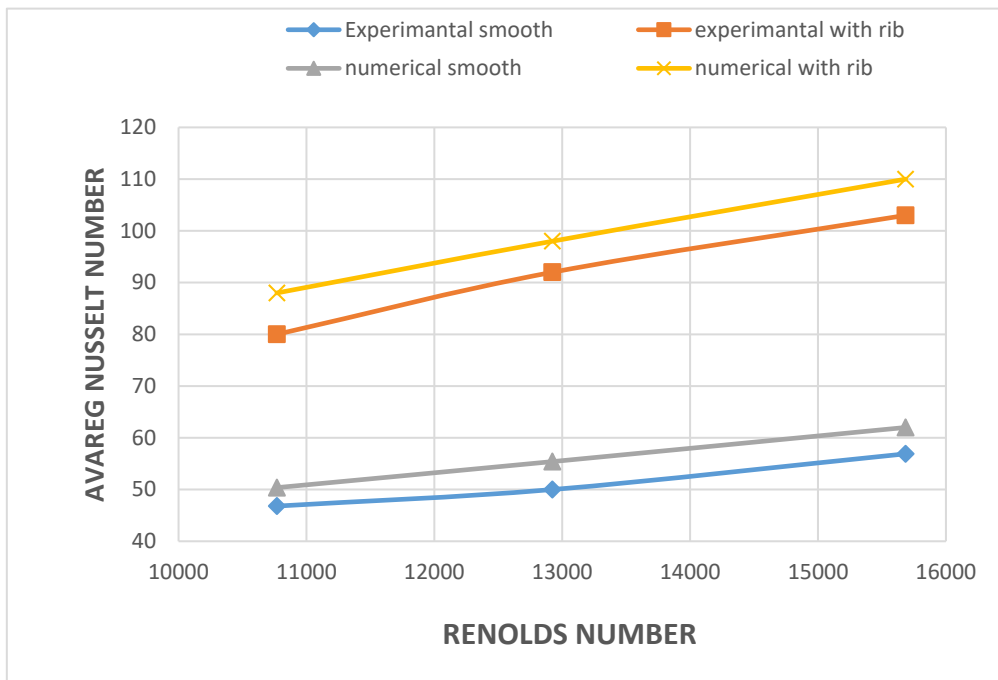


Figure 9. Experimental and numerical variations of average Nusselt number with Reynolds number

Figure (10) shows the contours of temperature distribution for the circular passage with circular ribs with sections of isosceles triangle at each rib location. After the first rib, air accelerates around the rib and boundary layer flow, with separation observed downstream of the ribs which creates vortices that enhance heat transfer.

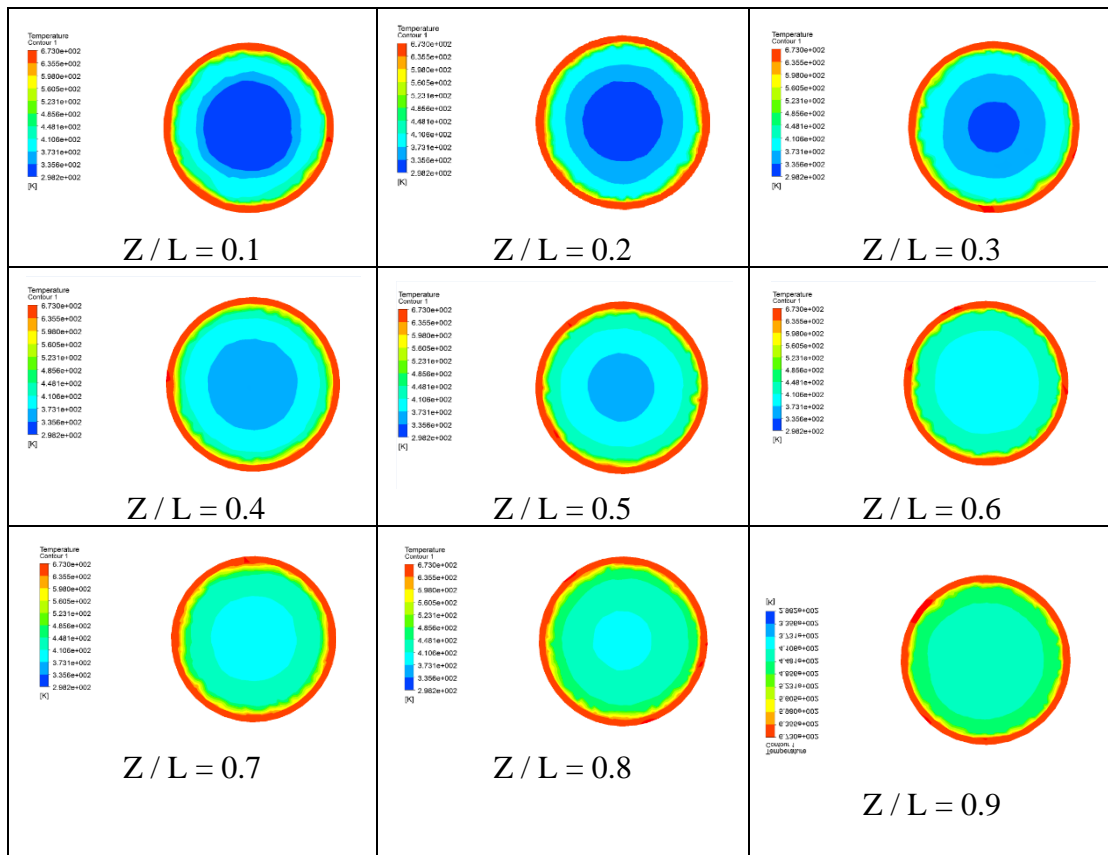


Figure 10. Temperature distribution at each rib location for ribbed circular passage

Figure (11) presents the contours of velocity distribution for a smooth circular passage; the cooling air velocity at the passage centreline decreases downstream constantly throughout the channel. Figure (12) shows the velocity distribution contour through a circular cross section with ribs, where the coolant air flow is accelerated and decelerated through the passage due to contraction and expansion caused by flow over the ribs.

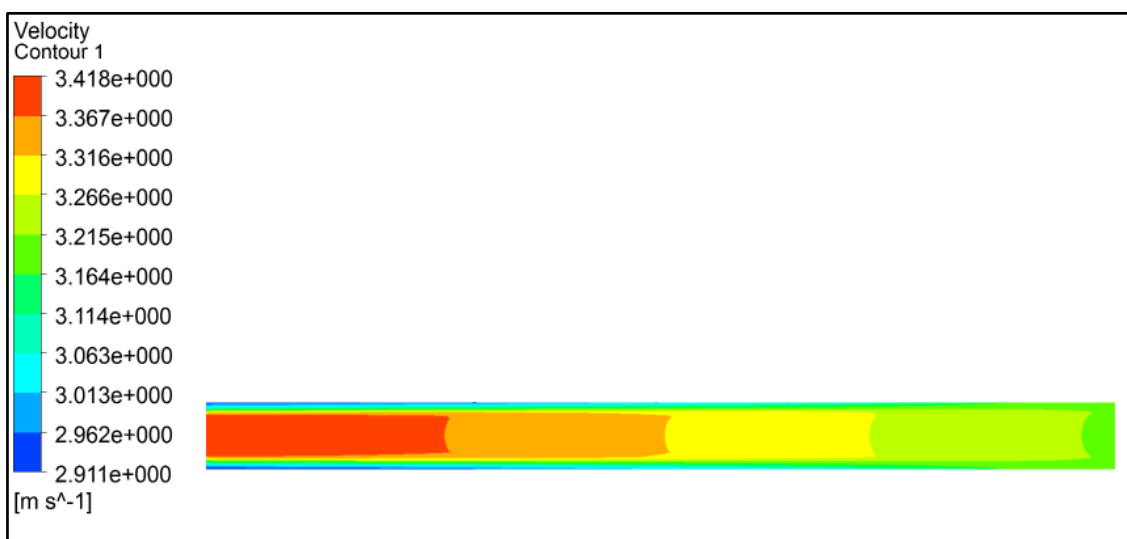


Figure 11. Velocity distribution for smooth circular passage

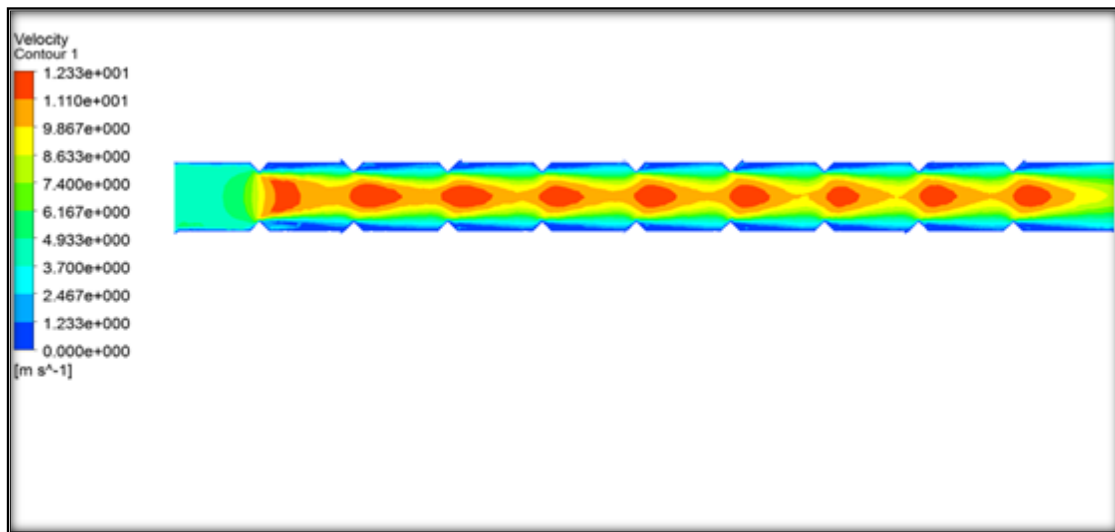


Figure 12. Velocity distribution for ribbed circular passage

Figures (13) presents the friction factor ratios for a constant surrounding hot air temperature of 673 K and Reynolds numbers $Re=10,800$, $12,900$, and $15,700$, respectively. The best case, with a lower pressure drop and higher heat transfer enhancement was case 2, $Re=12900$.



Figure 13 Experimental and numerical comparison of friction factor ratios with varying Reynolds numbers

From figure (14) it is clear that the average Nusselt number (Nu/Nu_0) for $Re=12,900$ is greater than for the other Reynolds numbers.

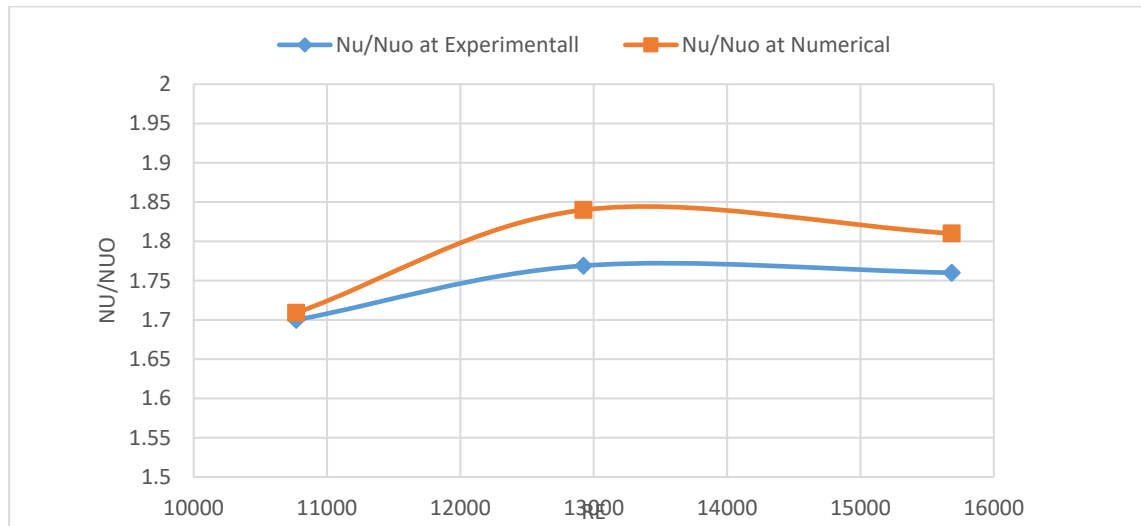


Figure 14. Experimental and numerical variation of average Nusselt number (Nu/Nu_0) with Reynolds number

As the average Nusselt number (Nu/Nu_0) for $Re=12,900$ is greater than for other Reynolds numbers, and the friction factor (f/f_0) is lower at this Reynolds number, the overall enhancement factor is best at this Reynolds number based on the enhancement factor equation.

Figure (15) presents the compound thermal performance for cases at constant surrounding air temperature of 673 K and coolant air flows of $Re=10,800$, 12,900, and 15,700, respectively. Case 2 ($Re=12,800$) shows the best results (lower pressure drop and higher heat transfer enhancement), while, case 3 ($Re=15,700$) shows the worst results (higher pressure drop and lower heat transfer). This means that the ribs in the latter case cause more obstacles to the flow while enhancing the heat transfer less.

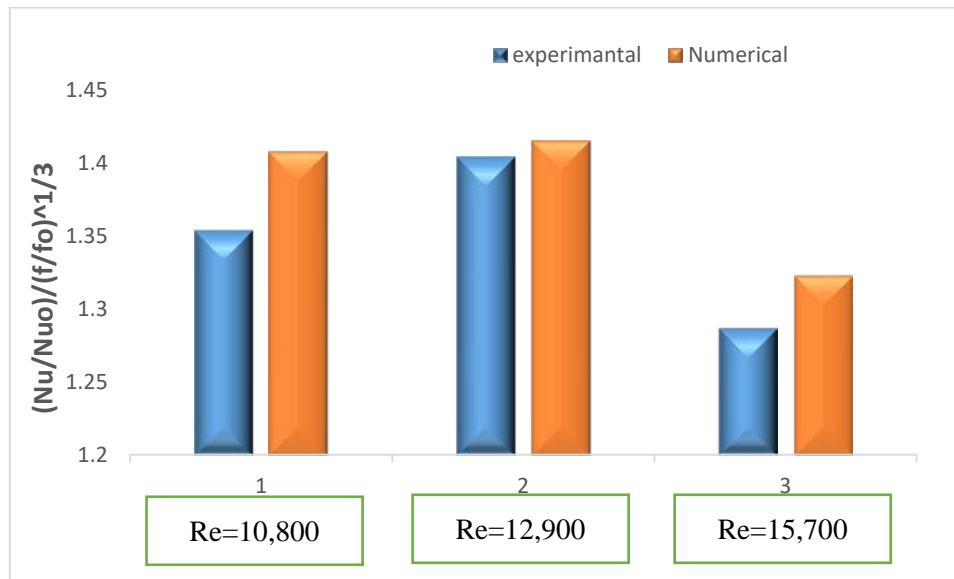


Figure 15. Experimental and numerical comparison of performance factor with different Reynolds numbers

6. Conclusions

1. The coolant air temperatures for passages with ribs were higher than those in the smooth duct by 10) % at Re=10,800, 9.6 % at Re=12,900 and 8.3% at Re=15,700.
2. The coolant air flow velocity accelerated and decelerated throughout the passages due to contraction and expansion by the ribs.
3. The heat transfer coefficient increased when ribs were used in the duct because of the increase in mixed flow (high turbulence) and increase in the surface area for heat transfer. The heat transfer coefficient was highest in case 2 at 84%.
5. The thermal performance factor along the passage is always larger than 1, meaning that each ribs configuration's performance exceeds that of the smooth passage.
6. A passage with ribs led to an increase in the coolant air temperature by 8.3%.
7. The enhancement performance factor for ribbed circular passage at Re=12,900 was equal to 1.4, which was the best-case scenario.

7. References

- [1] Han J-C J, Dutta S and Ekkad S 2012 *Gas turbine heat transfer and cooling technology* (New York: CRC Press ,Taylor & Francis, Inc)
- [2] Patel D K, Kamal P, Jain K, Dave R K, Prof A, Singh P and G P 2016 Heat Transfer Enhancement of Gas Turbine Blade'S Cooling Rectangular Channel With Internal Ribs of Different Rib Cross Sections Using Cfd *HEAT TRANSFER ENHANCEMENT OF GAS TURBINE BLADE'S COOLING RECTANGULAR CHANNEL WITH INTERNAL RIBS OF DIFFERENT RIB CROSS SECTIONS USING CFD*. pp 1818–24
- [3] Kumar S 2012 *Investigation of heat transfer and flow using ribs within gas turbine blade cooling passage: experimental and hybrid LES/RANS modeling* (The University of Wisconsin-Milwaukee)
- [4] Kumar H and Sehgal S S 2013 Study of Fluid Flow and Heat Transfer Through Mini-Channel Heat Sink *Asian J. Eng. Appl. Technol.* **2** 25–8
- [5] Karole S K, Singh I and Sonkusre P 2015 Heat Transfer and Friction Behaviors in Rectangular Duct with two Different Ribs *Int. J. Sci. Technol. Eng.* **1** 56–62
- [6] SHUKLA A 2009 *Forced Convection in Channels with Viscous Dissipation* (PhD Thesis)
- [7] Srivastava S and Saraogi M 2007 Electronic chip cooling in horizontal configuration using fluent-gambit
- [8] Rahmani R K, Tanbour E Y, Ayasoufi A and Molavi H 2014 Enhancement of Convective Heat Transfer in Internal Compressible *J. Enhanc. Heat Transf.* **2** 1–10
- [9] Hagari T, Ishida K, Takeishi K, Komiyama M and Oda Y 2016 Effect of Rib Density on Flow and Heat Transfer in an Internal Cooling Passage *ASME Turbo Expo 2016: Turbomachinery Technical Conference and Exposition* (American Society of Mechanical Engineers) p V05BT11A015-V05BT11A015
- [10] Metzger D E and Sahm M K 1985 Heat Transfer Around Sharp 180 Degree Turns in Smooth Rectangular Channels. *Am. Soc. Mech. Eng.* **108** 500–506
- [11] Carlomagno G M 1996 Quantitative infrared thermography in heat and fluid flow. Optical methods and data processing in heat and fluid flow *IMEchE Conference Transactions* vol 3 pp 279–90

- [12] Jian L, Xie G, Sunden B A, Wang L and Andersson M 2017 Enhancement of heat transfer in a square channel by roughened surfaces in rib-elements and turbulent flow manipulation *Int. J. Numer. Methods Heat Fluid Flow* **27** 1571–95
- [13] Sriromreun P and Sriromreun P 2017 Numerical study on heat transfer enhancement in a rectangular duct with incline shaped baffles *Chem. Eng. Trans.* **57**
- [14] Ugurlubilek N 2013 Numerical Heat Transfer and Turbulent Flow in a Circular Tube Fitted With Curvilinear Converging Rings *J. Therm. Sci. Technol.* **33** 111–8
- [15] Prof A and Hasan M R 2014 Numerical Investigation of Heat Transfer Enhancement in a Circular Tube Using Ribs of Separated Ports Assembly *Eur. Sci. Journal, ESJ* **2** 172–83
- [16] A. A, M.R. H and F.L R 2015 Numerical Investigation in a Circular Tube To Enhance Turbulent Heat Transfer Using Opened Rings -Triangular Cross Section *J. Babylon Univ. Sci.* **3**
- [17] Altaie A, Hasan M R and Rashid F L 2015 Numerical Investigation of Heat Transfer Enhancement in a Circular Tube with Rectangular Opened Rings *Bull. Electr. Eng. Informatics* **4** 18–25
- [18] A. A, M.R. H and F.L R 2015 Heat Transfer Enhancement in a Circular Tube Using Ribs with Middle Arm *Elixir Int. J.* **5**
- [19] Chung T J 2010 *Computational Fluid Dynamics* (New York: McGraw-Hill)
- [20] Han J-C, Dutta S and Ekkad S 2013 *Gas Turbine Heat Transfer and Cooling Technology* (New York: Taylor & Francis, Inc)